Solid State Ionics 53–56 (1992) 97–110
North-Holland

SOLID
STATE
IONICS

Non-Faradaic electrochemical modification of catalytic activity: the work function of metal electrodes in solid electrolyte cells

Costas G. Vayenas [1], Symeon Bebelis, Ioannis V. Yentekakis and Stelios Neophytides
Institute of Chemical Engineering and High Temperature Chemical Processes, and Department of Chemical Engineering, University of Patras, Patras GR-26110, Greece

The catalytic activity and selectivity of metal films used as electrodes in solid electrolyte cells can be altered dramatically and reversibly by polarizing the metal–solid electrolyte interface This effect, termed non-Faradaic electrochemical modification of catalytic activity (NEMCA) leads to steady state catalytic rate increases up to 3×10^5 times higher than the steady state rate of removal or supply of ions Catalytic rates can be enhanced reversibly up to 7000% The NEMCA effect has been already demonstrated with O^{2-} and Na^+ conducting solid electrolytes using Pt, Pd, Ag, Ni, Rh and Au electrodes In the present work we summarize some of the common experimental findings of previous studies and discuss the origin of NEMCA which lies in the controlled variation of the catalyst surface work function upon polarization of the catalyst–solid electrolyte interface We show both experimentally, using a Kelvin probe, and theoretically that in solid electrolyte cells there exists a one-to-one correlation between ohmic-drop-free electrode potential and gas-exposed electrode surface work function Thus solid electrolyte cells with metal electrodes can be used both to measure and to control the gas-exposed electrode work function This controlled variation in catalyst–electrode work function is due to ion spillover and results in significant variations in the binding strength of chemisorbed species, thus causing the NEMCA effect

1. Introduction

The interesting role that solid electrolyte cells can play in the study of heterogeneous catalysis was first recognized by Wagner [1] who proposed the use of such cells for the measurement of the activity of oxygen on metal catalysts. The experimental feasibility of this technique, which is usually called solid electrolyte potentiometry (SEP) has been demonstrated in a number of studies since 1979 [2–6], where kinetic and SEP measurements were combined to investigate the mechanism of several catalytic oxidations on metals. The SEP technique is particularly suitable for the study of oscillatory reactions [5,6].

More recently, a far more interesting and somehow surprising application of solid electrolyte cells in the area of heterogeneous catalysis was discovered. It had been known for some years that solid electrolyte cells operating in the oxygen "pump" mode can be used to carry out electrocatalytically several reactions such as NO decomposition [7,8], CO hydrogenation [9,10], methane conversion to C_2 hydrocarbons [11,12] and propylene conversion to acrolein [13]. The approach is similar in "Chemical Cogeneration" electrocatalytic studies [14–19]. In two studies involving ethylene and propylene epoxidation on Ag electrodes [20–22] it was observed that the behaviour was non-Faradaic, i.e., the increase in the rates of olefin epoxidation and conversion to CO_2 would typically exceed the rate of O^{2-} transport by a factor of 300, suggesting pronounced and reversible changes in the catalytic properties of the catalyst–electrode.

Very recently it has been shown that this new phenomenon of non-Faradaic electrochemical modification of catalytic activity (NEMCA) is not limited to any particular catalytic reaction, metal or solid electrolyte [23–37]. It was found that both catalytic activity and selectivity of metal films deposited on solid electrolytes can be altered in a dramatic, reversible and, to some extent, predictable manner [23–39]. This is achieved by carrying out the cat-

[1] To whom correspondence should be addressed at the current address Department of Chemical Engineering, Yale University, New Haven, CT 06520, USA.

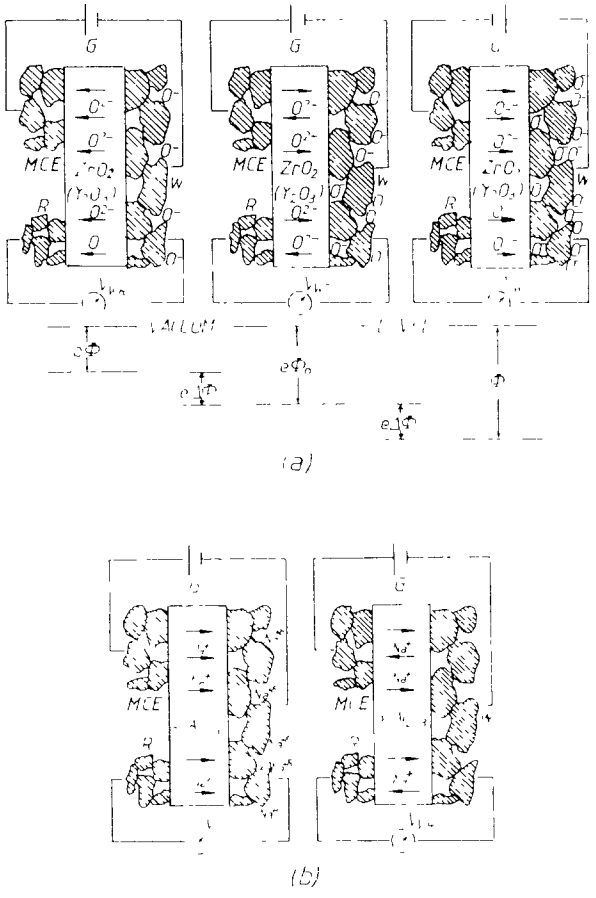

Fig 1 The principle of NEMCA When a metal counter electrode (MCE) is used in conjunction with a galvanostat (G) to supply or remove ions (O^{2-} for the doped ZrO_2 (a), Na^+ for β''-Al_2O_3 (b)) to or from the polarizable solid electrolyte/catalyst (or working electrode, W) interface, spillover ions (O^- in (a), $Na^{\delta+}$ in (b)) together with their compensating charge in the metal are produced or consumed at the tpb between the three phases solid electrolyte/catalyst/gas This causes an increase (right) or decrease (left) in the work function $e\Phi$ of the gas-exposed catalyst surface In all cases $\Delta e\Phi = e\Delta V_{WR}$ where ΔV_{WR} is the overpotential measured between the catalyst and the reference electrode (R)

alytic reaction in solid electrolyte cells of the type gaseous reactants, metal catalyst|solid electrolyte|metal, O_2 and by using a galvanostat or potentiostat to polarize the metal–solid electrolyte interface by, typically, 0 1 to 1 V. This is shown schematically in fig 1.

The term non-Faradaic electrochemical modification of catalytic activity (NEMCA) has been used to describe this new phenomenon, since the steady-state catalytic rate increase can be up to a factor of 3×10^5 higher than the steady-state rate of ion transfer through the solid electrolyte [23,25,26,30,38]

The observed dramatic changes in the catalytic rate are up to a factor of 70 higher than the normal (open-circuit) catalytic rate [23,36,38]. Significant changes in product selectivity have also been observed [23–39].

The NEMCA effect can be viewed as a special case of catalyst promotion [40], i e , *the solid electrolyte serves as an active catalyst support* which can modify dramatically the catalytic properties of metals via ion spillover. This new application could eventually become of technological importance for solid electrolyte cells [39], in addition to their current uses as sensors [41] and as fuel cells [42] In the present work we summarize the main common findings of previous NEMCA studies [23–39] and discuss the origin of NEMCA

2. Experimental

The catalytic reactor shown in fig. 2a contains a solid electrolyte tube and has been described in detail elsewhere [24,26,27]. Two types of solid electrolyte were used, i.e., fully stabilized zirconia (8 mol% Y_2O_3) and β'-Al_2O_3. The three-electrode configuration shown in fig. 2b was used in conjunction with the current interruption technique and a recording oscilloscope to measure accurately the catalyst electrode overpotential $\eta=\Delta V_{WR}$, where V_{WR} is

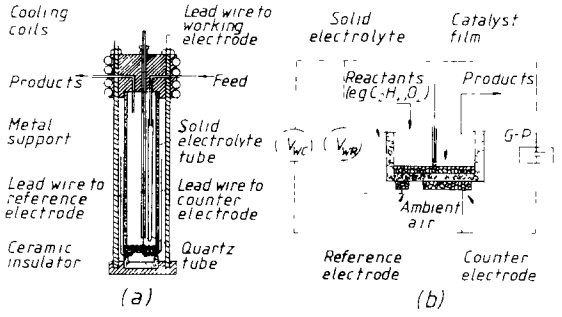

Fig 2 Solid electrolyte catalytic reactor for NEMCA studies (a) and configuration of catalyst and auxiliary electrodes (b), G–P galvanostat–potentiostat

the ohmic-drop-free catalyst potential (W stands for working electrode) versus a reference (R) electrode, as described in detail elsewhere [24,26,27].

Upon cell polarization the current I is defined positive when O^{2-} are pumped to or Na^+ removed from the catalyst electrode. The gas feed and analysis unit, utilizing on-line gas chromatography, mass spectrometry and IR spectroscopy, has also been described in previous papers [23–39] where catalyst and auxiliary electrodes preparation and characterization details are presented. It is worth emphasizing that the catalyst film must be sintered at elevated temperatures (e g. 850°C for Pt, 680°C for Ag) to ensure a low I_0, i.e. highly polarizable metal–solid electrolyte interface [26,27,38]. Porous metal films used in NEMCA studies are typically 5 to 10 μm thick, have superficial surface areas of 1–2 cm^2 and true surface areas of 50–500 cm^2 as measured by means of surface titration techniques [24–38].

The catalyst work function $e\Phi$ was measured in situ by using a Kelvin probe (Besocke/Delta Phi-Electronic, probe "S") with a 2.5 mm diameter Au-grid vibrating condenser element placed ~500 μm from the catalyst surface. A slightly different electrode configuration was used in these experiments [33,35]. It was verified that the work function measurements were not influenced by the exact distance of the two condenser elements.

3. General features of the NEMCA effect

Table 1 lists the catalytic reactions which have been studied so far and have been shown to exhibit NEMCA. In order to compare different catalytic reactions it is useful to define two quantities, i.e., the enhancement factor Λ and the rate enhancement ratio ρ. The former quantity is defined from

$$\Lambda = \Delta r(\text{catalytic})/(I/nF)\,, \qquad (1)$$

where Δr (catalytic) is the change in the rate of the catalytic reaction and I/nF is the rate of ion transport to or from the catalyst (n is the ion charge). A reaction exhibits the NEMCA effect when $|\Lambda| \gg 1$.

Table 1
Catalytic reactions found to exhibit the NEMCA effect

Reactants	Products	Catalyst	Electrolyte	T (°C)	Λ	$\rho = r/r_o$
I. Positive (electrophobic) NEMCA effect ($\Delta r > 0$ with $I > 0$ [a], $e\Delta\Phi > 0$)						
C_2H_4, O_2	C_2H_4O, CO_2	Ag	ZrO_2–Y_2O_3	320–470	[0, 300]	<3 [b]
C_3H_6, O_2	C_3H_6O, CO_2	Ag	ZrO_2–Y_2O_3	320–420	[0, 300]	<2 [b]
C_2H_4, O_2	CO_2	Pt	ZrO_2–Y_2O_3	260–450	[0, 3×10^5]	<55
C_2H_4, O_2	CO_2	Pt	β″-Al_2O_3	180–300	[0, 5×10^4]	<4
CO, O_2	CO_2	Pt	ZrO_2–Y_2O_3	300–550	[0, 2×10^3]	<3
CO, O_2	CO_2	Pd	ZrO_2–Y_2O_3	400–550	[0, 10^3]	<1 5
CH_3OH, O_2	H_2CO, CO_2	Pt	ZrO_2–Y_2O_3	300–500	[0, 10^4]	<4 [b]
CH_4, O_2	CO_2, C_2H_4, C_2H_6	Ag	ZrO_2–Y_2O_3	650–850	[0, 5]	<30 [b]
CH_4, O_2,	CO_2	Pt	ZrO_2–Y_2O_3	600–750	[0, 5]	<70 [b]
CO, O_2	CO_2	Ag	ZrO_2–Y_2O_3	350–450	[0, 20]	<5
C_2H_4, O_2	C_2H_4O, CO_2	Ag	β″-Al_2O_3	350–410	[0, 3×10^3]	<3 [b]
CO_2, H_2	CH_4, CO	Rh	ZrO_2–Y_2O_3	390–450	[0, 40]	<2 [b]
CH_4, H_2O	CO, CO_2, H_2	Ni	ZrO_2–Y_2O_3	600–900	[0, 3]	<2 [b]
II Negative (electrophilic NEMCA effect $\Delta r > 0$ with $I < 0$ [a], $e\Delta\Phi < 0$)						
CO, O_2	CO_2	Pt	ZrO_2–Y_2O_3	300–550	[0, −500]	<6
CH_3OH, O_2	H_2CO, CO_2	Pt	ZrO_2–Y_2O_3	300–550	[0, -10^4]	<15 [b]
CH_3OH	H_2CO, CO, CH_4	Ag	ZrO_2–Y_2O_3	550–750	[0, −25]	<6 [b]
CH_3OH	H_2CO, CO, CH_4	Pt	ZrO_2–Y_2O_3	300–500	[0, −10]	<3 [b]
CH_4, O_2	CO_2	Pt	ZrO_2–Y_2O_3	600–750	[0, −5]	<30
CO, O_2	CO_2	Ag	ZrO_2–Y_2O_3	350–450	[0, −800]	<15

[a] Current is defined positive when O^{2-} are supplied to or Na^+ removed from the catalyst surface
[b] Change in product selectivity observed

When $\Lambda > 1$, the reaction is said to exhibit positive or electrophobic NEMCA behaviour. When $\Lambda < -1$ the reaction is said to exhibit negative or electrophilic NEMCA behaviour [23–39].

The rate enhancement ratio ρ is defined from

$$\rho = r(\text{catalytic})/r_o(\text{catalytic}), \quad (2)$$

where r_o denotes the regular, i.e., open-circuit, catalytic rate.

Despite the differences in open-circuit catalytic behaviour of the catalytic reactions shown in table 1 and the dramatic differences in the observed Λ and ρ values, there are three common features of NEMCA which have been observed in all the systems studied so far. These features can be summarized as follows.

(i) Catalytic rates depend exponentially on the ohmic-drop-free catalyst potential V_{WR}:

$$\ln(r/r_o) = \alpha e(V_{WR} - V^*_{WR})/k_B T, \quad (3)$$

where k_B is Boltzmann's constant and α and V^*_{WR} are reaction and catalyst-specific constants The parameter α typically takes values between -1 and 1 and determines the electrophobicity ($\alpha > 0$) or electrophilicity ($\alpha < 0$) of a catalytic reaction [23,38]. As recently shown experimentally [23,25] and as analyzed in detail in the present work, cell polarization induces a change $\Delta e\Phi$ in the work function $e\Phi$ of the gas-exposed catalyst surface which is equal to $e\Delta V_{WR}$, where ΔV_{WR} is the change in the ohmic-drop-free catalyst potential. This implies that eq. (3) can also be written as:

$$\ln(r/r_o) = \alpha e(\Phi - \Phi^*)/k_B T, \quad (4)$$

where Φ^* is, again, a catalyst- and reaction-specific constant. Some examples are given in fig. 3 for a number of Pt-catalyzed oxidations. Eq. (4) is found to hold over wide ranges of $e\Phi$, typically 0.3 to 1 eV. Over the same $e\Phi$ ranges catalytic activation energies are found to vary linearly with $e\Phi$ [38].

(ii) The order of magnitude of the absolute value $|\Lambda|$ of the enhancement factor Λ for any catalytic reaction can be estimated from

$$|\Lambda| = 2Fr_o/I_o, \quad (5)$$

where I_o is the exchange current of the catalyst–solid electrolyte interface, which can be measured from standard Tafel plots [26,27]. The theoretical derivation of eq. (5) has been presented elsewhere

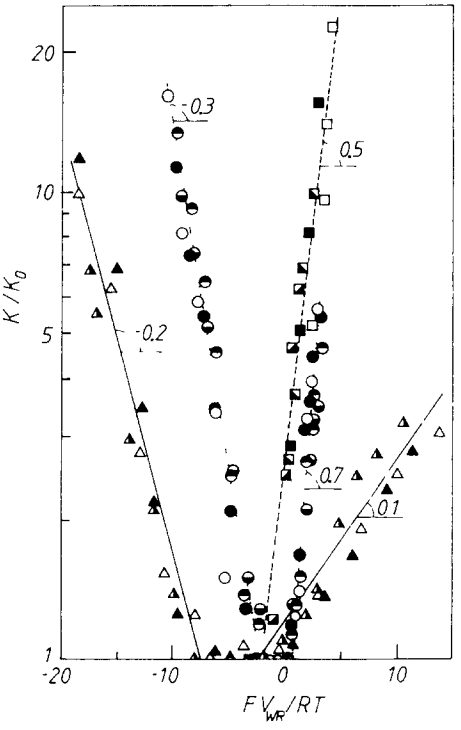

Fig 3 Effect of catalyst potential V_{WR} and work function $e\Phi$ on the kinetic rate constant K for CO_2 production in the catalytic systems (a) CH_3OH, O_2, Pt|ZrO_2 (8 mol% Y_2O_3) $P_{CH_3OH} = 0.9$ kPa, $P_{O_2} = 19$ kPa, (△) $T = 353$°C, (▲) $T = 377$°C, (◮), $T = 425$°C, (b) CH_4, O_2, Pt/ZrO_2 (8 mol% Y_2O_3) $P_{CH_4} = 2$ kPa, $P_{O_2} = 2$ kPa, (○) $T = 650$°C, (◓) $T = 700$°C, (●) $T = 675$°C, (◒) $T = 730$°C (c) C_2H_4, O_2, Pt/ZrO_2 (8 mol% Y_2O_3) $P_{C_2H_4} = 0.4$ kPa, $P_{O_2} = 4.8$ kPa, (□) $T = 296$°C, (■) $T = 324$°C, (◧) $T = 360$°C, (◪) $T = 399$°C, $\Delta e\Phi = 0$ corresponds to Pt in equilibrium with $P_{O_2} = 21$ kPa

[26,38] As shown in fig. 4 there is excellent agreement between eq. (5) and experiment over at least five orders of magnitude. Eq. (5) underlines the fact that in order to obtain a strong non-Faradaic rate enhancement, i.e. $|\Lambda| \gg 1$, one has to use a highly polarizable, i e. low I_o, catalyst–solid electrolyte interface

(iii) The catalytic rate relaxation time τ during galvanostatic transients, defined as the time required for the NEMCA-induced change in catalytic reaction rate to reach 63% of its final steady-state value, can be estimated from.

$$\tau \approx 2FN/I, \quad (6)$$

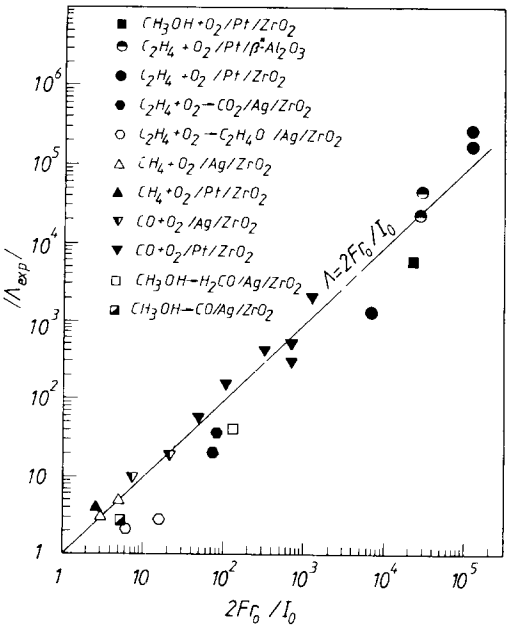

Fig 4 Comparison of predicted and measured enhancement factor Λ values for the catalytic reactions already found to exhibit the NEMCA effect (table 1)

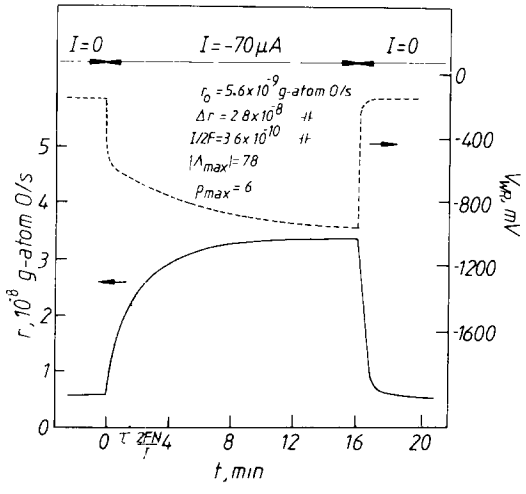

Fig 5 Transient response of catalytic rate and catalyst potential upon current application and interruption during CO oxidation on $Ag/ZrO_2(Y_2O_3)$, $T=415°C$, $P_{O_2}=3$ kPa, $P_{CO}=5$ kPa, $N=5.8\times10^{-8}$ g-atom O

when using O^{2-}-conducting solid electrolytes and from:

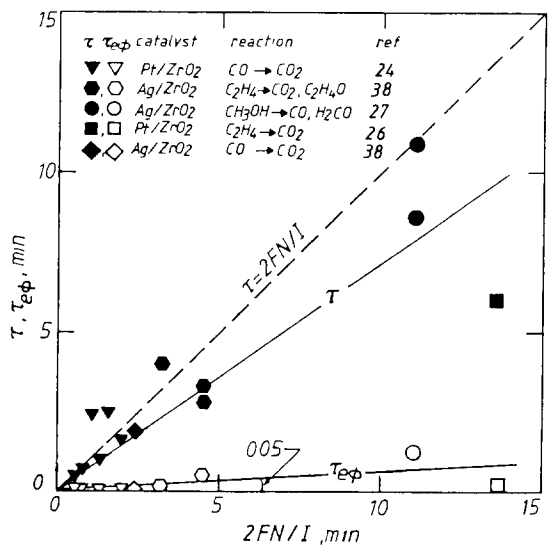

Fig 6 Dependence of the catalytic rate relaxation time constant τ (filled symbols) and of the catalyst potential and work function time constant (open symbols) on 2FN/I during NEMCA galvanostatic transients of catalyst films deposited on stabilized ZrO_2

$$\tau \approx FN\theta_{Na}/I\,, \tag{7}$$

when using Na^+-conducting solid electrolytes, where N is the metal catalyst surface area expressed in g-atom and θ_{Na} is the, coulometrically determined, Na coverage on the catalyst surface. An example is given in fig. 5 for the case of CO oxidation on $Ag/ZO_2(Y_2O_3)$ [37].

The validity of eq. (6) is demonstrated in fig. 6 which compares measured τ values for a number of reactions with $2FN/I$. As shown in fig. 6, but also in fig. 5, the time $\tau_{e\Phi}$ required for ΔV_{WR} or, equivalently [38] $\Delta e\Phi$ to reach 63% of its steady-state value is considerably shorter than τ as analyzed in detail elsewhere [38].

4. Origin of NEMCA: The work function of catalyst films deposited on solid electrolytes

Very recent experimental work utilizing a Kelvin probe to measure in situ the work function of catalyst films deposited on solid electrolytes [35] has shown that:

(1) Solid electrolyte cells can be used to alter significantly the work function $e\Phi$ of the gas-exposed,

i.e., catalytically active, catalyst electrode surface by polarizing the catalyst-solid electrolyte interface.

(ii) Solid electrolyte cells are work function probes for the gas-exposed, catalytically active catalyst-electrode surfaces, i.e the change $\Delta e\Phi$ in catalyst surface average work function $e\Phi$ is equal to $e\Delta V_{WR}$. The catalyst potential V_{WR} with respect to a reference electrode can be varied both by changing the gaseous composition and/or by polarizing the catalyst–solid electrolyte interface.

The above two observations play a key role in understanding and interpreting the NEMCA effect and it is therefore important to provide a rigorous theoretical explanation for them.

We start by considering a schematic representation of a porous metal film deposited on a solid electrolyte, e.g., on Y_2O_3-stabilized-ZrO_2 (fig. 7). The catalyst surface is divided in two distinct parts: One part, with a surface area A_E is in contact with the electrolyte. The other with a surface area A_C is not in contact with the electrolyte It constitutes the gas-exposed, i.e., catalytically active film surface area. *Catalytic reactions* take place on this surface only. In the subsequent discussion we will use the subscripts E (for electrochemistry) and C (for catalysis), respectively, to denote these two distinct parts of the catalyst film surface. Regions E and C are separated by the three-phase-boundaries (tpb) where *electrocatalytic reactions* take place Since electrocatalytic reactions can also take place to, usually, a minor extent on region E [43], one may consider the tpb to be part of region E as well. It will become apparent below that the essence of NEMCA is the following One uses electrochemistry (i.e. a slow electrocatalytic reaction) to alter the electronic properties of the metal–solid electrolyte interface E. This perturba-

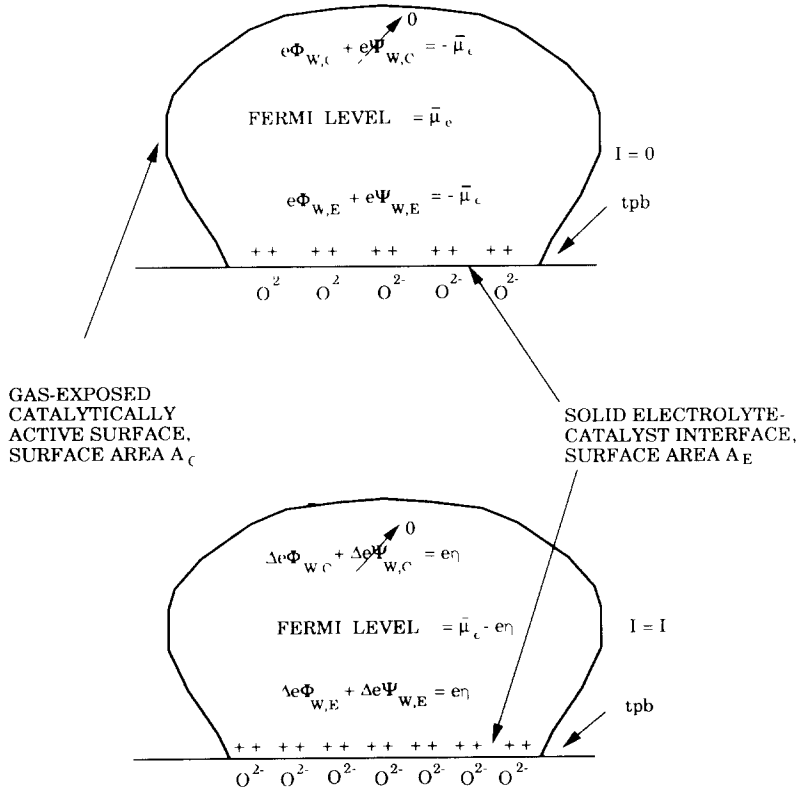

Fig 7 Schematic representation of a metal crystallite deposited on YSZ and of the changes induced in its electronic properties upon polarizing the catalyst-solid electrolyte interface and changing the Fermi level (or electro-chemical potential of electrons) from an initial value $\bar{\mu}$ to a new value $\bar{\mu} - e\eta$.

tion is then propagated via the spatial constancy of the Fermi level E_F throughout the metal film to the metal–gas interface C, altering its electronic properties and thus influencing catalysis, i.e. catalytic reactions taking place on the metal-gas interface C.

We then concentrate on the meaning of V_{WR}, i.e., of the (ohmic-drop-free) potential difference between the catalyst film (W, for working electrode) and the reference film (R). The measured (by a voltmeter), potential difference V_{WR} is, by definition [44], the difference in the inner (or Galvani) potentials φ of two electrodes:

$$V_{WR}=\varphi_W-\varphi_R\,. \tag{8}$$

The Galvani potential is the electrostatic potential of electrons inside the metal film. The electrochemical potential of electrons in a metal $\bar{\mu}$ is related to φ via:

$$\bar{\mu}=\mu+(-e)\varphi\,, \tag{9}$$

where μ is the chemical potential of electrons in the metal, a purely bulk property. It is worth reminding that $\bar{\mu}$ can be shown [45,46] to be identical with the Fermi level E_F in the metal (fig. 8 and refs. [45–50] which provide an excellent introduction to the meaning of the various potentials discussed here). In view of eq. (9) one can rewrite eq. (8) as:

$$eV_{WR}=\bar{\mu}_R-\bar{\mu}_W+(\mu_W-\mu_R)\,. \tag{10}$$

Eq. (10) represents the electrochemical way of counting the energy difference between zero (defined in the present discussion as the potential energy of an electron at its ground state at "infinite" distance from the metal [44]) and the Fermi level E_F. The latter must not be confused with the Fermi energy [μ] which is the energy difference between the Fermi level and the energy at the bottom of the conduction band and provides a measure of the average kinetic energy of electrons at the Fermi level (fig. 8). The electrochemical way of splitting the energy difference from zero to E_F is a conceptual one, as the absolute values of φ and μ are not accessible to direct experimental measurement. The second way to split this energy difference is to consider it as the sum of the work function $e\Phi$ (Φ is the electron extraction potential) and of $e\Psi$, where Ψ is the outer (or Volta) potential (figs. 8 and 9).

The work function $e\Phi$ is the work required to bring an electron from the Fermi level of the metal to a point outside the metal where the image forces are negligible, i.e., typically 10^{-4} to 10^{-5} cm outside the metal surface [44,47,48]. The Volta potential Ψ at this point is defined so that the energy required to bring an electron from that point to an "infinite" distance from the metal surface is $e\Psi$:

$$\bar{\mu}=-e\Phi-e\Psi\,. \tag{11}$$

Needless to say that $e\Phi$ and Ψ (which are both accessible to experimental measurement) are not, in general, spatially uniform over the metal surface. Different crystallographic planes are well known to have different $e\Phi$ values and thus non-trivial variations in $e\Phi$ and $e\Psi$ are to be expected on the surface of polycrystalline samples. It is important, however, to notice that their sum has to be spatially uniform (eq. (11)) since the electrochemical potential $\bar{\mu}$ or, equivalent, Fermi level E_F is spatially uniform. This is true even when an electrical current is passing through the metal film under consideration, provided that the ohmic drop in the film is negligible (less than a few mV) which is always the case with the conductive metal films and low currents employed in NEMCA studies. It is also important to notice that, by definition, Ψ vanishes if there is no *net* charge on the metal surface under consideration.

One can then combine eqs. (10) and (11) to obtain:

$$eV_{WR}=e\Phi_W-e\Phi_R+e(\Psi_W-\Psi_R)+(\mu_W-\mu_R)\,. \tag{12}$$

It is worth emphasizing that eq. (12) is valid under both open-circuit and closed-circuit conditions and that it holds for *any* part of the surfaces of the catalyst and the reference electrodes. Thus, referring to the metal electrode surfaces in contact with the electrolyte (region E) it is:

$$eV_{WR}=e\Phi_{W,E}-e\Phi_{R,E}+e(\Psi_{W,E}-\Psi_{R,E})+(\mu_W-\mu_R)\,, \tag{13}$$

while for the gas-exposed, i.e., catalytically active electrode surfaces (region C) it is:

$$eV_{WR}=e\Phi_{W,C}-e\Phi_{R,C}+e(\Psi_{W,C}-\Psi_{R,C})+(\mu_W-\mu_R)\,. \tag{14}$$

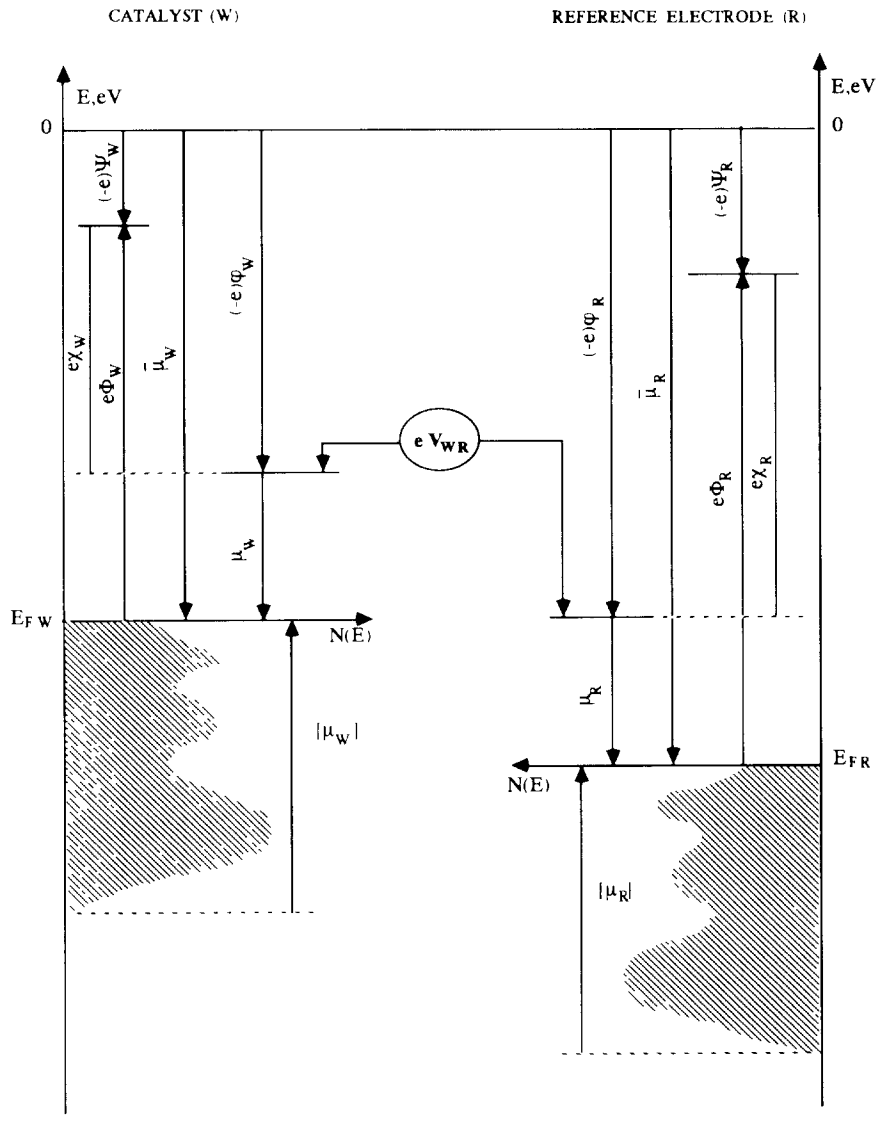

Fig 8 Schematic representation of the density of states $N(E)$ in the conduction band and of the definitions of work function $e\Phi$, chemical potential of electrons μ, electrochemical potential of electrons or Fermi level $\bar{\mu}$, surface potential χ Galvani (or inner) potential φ, Volta (or outer) potential Ψ, Fermi energy $[\mu]$ for the catalyst (W) and for the reference electrode (R) The measured potential difference V_{WR} is by definition the difference in Galvani potentials, φ, μ and $\bar{\mu}$ are spatially uniform, $e\Phi$ and Ψ can vary locally on the metal sample surfaces, and the Ψ potentials vanish, on the average, for the gas-exposed catalyst and reference electrode surfaces

In order to understand the origin of NEMCA one needs to concentrate only on eq. (14) which refers to the gas-exposed, catalytically active, film surface As already stated, different crystallographic planes will, in general, have different $e\Phi$ values, thus, even over region C the work function $e\Phi$ need not be spatially uniform. These local spatial variations in $e\Phi$ and Ψ are not expected to be significant in polycrystalline films with large (~ 1 μm) crystallites such as the ones used in most NEMCA studies [23–39] since the surface must consist primarily of low Miller index planes, e g. of the (111) plane in the case of Pt films [38]. This is also supported by recent STM information [38] We will thus first assume that $e\Phi$

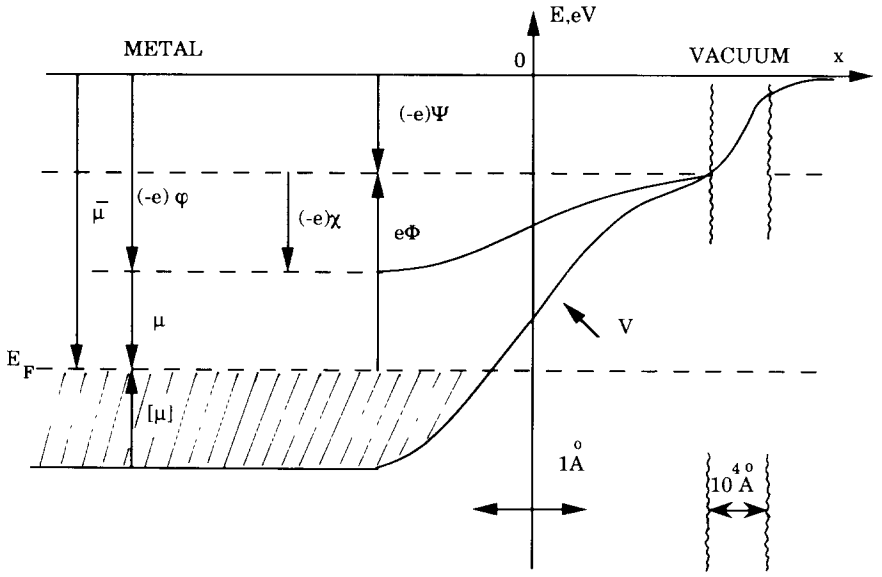

Fig 9 Schematic representations of the definitions of work function $e\Phi$, chemical potential of electrons μ, electrochemical potential of electrons or Fermi level $\bar{\mu}=E_F$, surface potential χ, Galvani (or inner) potential φ, Volta (or outer) potential Ψ, Fermi energy $[\mu]$ and of the variation in the mean effective potential energy V of electrons in the vicinity of a metal-vacuum interface according to the jellium model (based on refs [38,50])

and Ψ are spatially uniform over region C and will treat the more general case below. Returning to eq. (14) we note that when V_{WR} is changed by ΔV_{WR} by varying the gaseous composition over the catalyst or by polarizing by means of a current the catalyst–solid electrolyte interface, then the properties of the reference electrode remain unaffected and μ_W which is pure bulk property also remains constant, therefore:

$$e\Delta V_{WR} = \Delta e\Phi_{W,C} + e\Delta\Psi_{W\,C} . \qquad (15)$$

We then concentrate on the Volta potential terms $\Psi_{W,C}$ and $\Delta\Psi_{W\,C}$. Can they be non-zero? There may very well be a small net charge on the catalyst film, i.e., on its surface, but where will it be localized? In region E, in region C or in both? It follows from simple electrostatic considerations and taking into account that the solid electrolyte has an abundance of charge carriers while the gas phase does not have any, that all the net charge in the metal will be localized in region E facing an equal and opposite charge in the solid electrolyte. To further elucidate this point in a simplistic point of view consider the, initially uncharged, metal film brought into contact with the also initially uncharged, solid electrolyte. When the film and the solid electrolyte are brought in contact the system has to remain neutral Thus if a charge q develops in the film a charge $-q$ will develop in the solid electrolyte facing the metal [44]. Thus if the film charge q were to be split to a part q_E remaining in region E and a part q_C developing in region C then a net charge $-(q-q_E)=-q_C$ would remain in region E attracting the charge q_C back in region E. Thus no *net* charge can be sustained in region C, therefore $\Psi_{W\,C}=0$ under both open-circuit and closed-circuit conditions.

One can then rewrite eqs. (14) and (15) as:

$$eV_{WR} = e\Phi_{W,C} - e\Phi_{R\,C} + (\mu_W - \mu_R) , \qquad (16)$$

$$e\Delta V_{WR} = \Delta e\Phi_{W\,C} . \qquad (17)$$

It is worth noting that if the reference electrode is of the same bulk material with the catalyst and are both at the same temperature, then $\mu_W=\mu_R$. Using the superscript "o" to denote open-circuit conditions ($I=0$), one can rewrite eq. (16) as:

$$eV^{o}_{WR} = e\Phi_{W,C} - e\Phi_{R,C} . \qquad (18)$$

Eq. (18) shows that the EMF eV^{o}_{WR} of solid elec-

trolyte cells with electrodes made of the same bulk material provides a direct measure of the difference in work function of the gas-exposed, i e., catalytically active, electrode surfaces. Thus, *solid electrolyte cells are work function probes for their gas exposed electrode surfaces.*

Eq. (17) is equally important, as it shows that the work function of the catalytically active catalyst electrode surface can be varied at will by varying the (ohmic-drop-free) catalyst potential. This can be done either by varying the gaseous composition over the catalyst or by using a potentiostat Catalytic chemists would clearly anticipate the former mode: When the gaseous composition changes, then surface coverages will change with a concomitant change in work function. But what about the latter? For the work function to change something must have changed on the surface. What can be changed on the gas-exposed surface by means of a potentiostat? As discussed in detail elsewhere [38] there is a strong and convincing experimental evidence that the work function change on the surface is due to spillover ions originating from the solid electrolyte. This is also supported by in situ XPS measurements which have shown the appearance of O 1s signal corresponding to ionically bonded oxygen on Ag films subject to O^{2-} pumping in stabilized zirconia cells [49,50] These spillover ions (oxygen anions for the case of doped ZrO_2, partly ionized Na for the case of β''-Al_2O_3) accompanied by their compensating charge in the metal thus forming spillover dipoles, spread over the catalytically active surface altering its work function and catalytic properties (fig. 1).

One can then address the question of the meaning of eqs. (17) and (18) in the case of significant spatial variations in the work function $e\Phi$ of the polycrystalline catalyst surface. In this case, due to the constancy of the Fermi level, slightly different nonzero excess free charge densities will exist on different planes with different $e\Phi$, causing local variations in Ψ. Surface physicists would refer to this as a local variation in the "vacuum level" In this case the average surface work function $e\Phi$ is defined from [48]:

$$e\Phi = \sum_j f_j e\Phi_j , \qquad (19)$$

where f_j is the total catalyst surface fraction corresponding to a crystallographic plane with a work function $e\Phi_j$. One can then apply eq. (14) to each crystallographic plane j:

$$eV_{WR} = e\Phi_{W(C,j)} - e\Phi_{R(C)} + e(\Psi_{W(C,j)} - \Psi_{R(C)}) , \qquad (20)$$

where for simplicity it is assumed that the reference electrode is of the same material with the catalyst ($\mu_W = \mu_R$). By multiplying eq (20) by f_j, summing for all planes and noting that $\Psi_{R,C} = 0$ one obtains:

$$eV_{WR} = \sum_j f_j e\Phi_{W(C,j)} - e\Phi_{R(C)} + \sum_j f_j e\Psi_{W(C,j)} \qquad (21)$$

Since Ψ is proportional to the local excess free charge it follows that the term $\sum f_j e\Psi_{W,C,j}$ is proportional to the net charge stored in the metal in region C. This net charge, however, was shown above to vanish, consequently $\sum f_j e\Psi_{W,C,j}$ must also vanish.

Consequently eq. (21) takes the same form as eq. (18) where, now, $e\Phi$ stands for the average surface work function. The same holds for eq. (17)

5. Results

As shown in figs 10 and 11a, eqs. (17) and (18) have been recently verified by directly measuring the work function of catalyst electrodes using a Kelvin probe (vibrating condenser method) under reaction conditions [23,35].

Fig. 10 shows that the change in the work function of the gas-exposed (that is, catalytically active) surface of the catalyst is $e\Delta V_{WR}$, both under closed- and open-circuit conditions In the former case V_{WR} was varied by changing the polarizing current with the catalyst exposed to air or to $NH_3/O_2/He$ and $CO/O_2/He$ mixtures, whereas in the latter only the gaseous composition was varied Both doped ZrO_2 and β''-Al_2O_3 solid electrolytes were used

As shown in fig. 11 the equality $\Delta e\Phi = e\Delta V_{WR}$ also holds to a good approximation during transients In this case a constant current is applied at $t=0$ between the catalyst and the counter electrode and one follows the time evolution of V_{WR} by a voltmeter and of $e\Phi$ by a Kelvin probe

Work function transients of the type shown in fig 11 can be used to estimate initial dipole moments of the spillover dipoles on the catalyst surface [33,35]

Thus referring to Na supply onto a Pt catalyst surface with surface area A_C via a β''-Al_2O_3 solid elec-

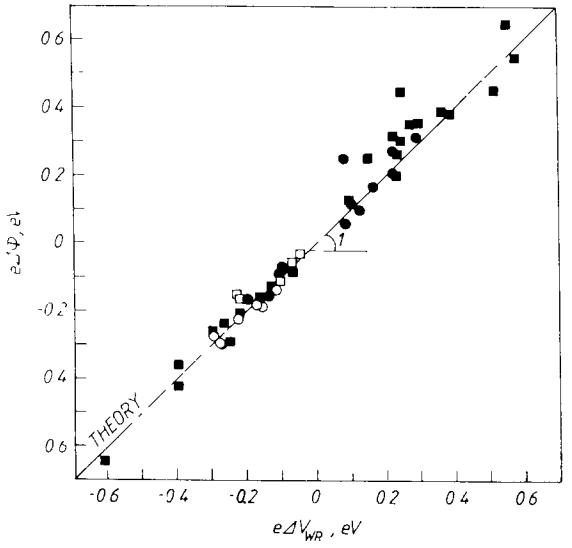

Fig 10 Steady state effect of the change in the ohmic-drop-free catalyst potential V_{WR} on catalyst surface work function $e\Phi$, squares Y_2O_3-doped-ZrO_2 electrolyte, $T=300°C$, circles β''-Al_2O_3 electrolyte, $T=240°C$, filled symbols closed-circuit operation, open symbols open circuit operation [35]

trolyte, one can use Faraday's law to obtain:

$$\frac{d\theta_{Na}}{dt} = -\frac{N_{AV}(I/2F)}{A_C N_{Pt}}, \tag{22}$$

where N_{AV} is Avogadro's number and $N_{Pt}=1.53\times10^{19}$ atoms/m^2 is the surface Pt concentration on the Pt(111) plane. One can then combine eq. (22) with the definition of the Na coverage θ_{Na} ($=N_{Na}/N_{Pt}$) and with the differential form of the Helmholz equation:

$$\frac{d(e\Phi)}{dt} = -\frac{eP_0}{\epsilon_0}\frac{dN_{Na}}{dt}, \tag{23}$$

where N_{Na} denotes adsorbed Na atoms/m^2, $\epsilon_0=8.85\times10^{-12}$ C^2/J m and P_0 is the initial dipole moment of Na on Pt to obtain:

$$\frac{d(e\Phi)}{dt} = \frac{P_0 I}{\epsilon_0 A_C}. \tag{24}$$

Using eq. (24) and the initial slope in fig. 11 one computes the initial dipole moment P_0 of Na on Pt to be 2.15×10^{-29} C·m or 6.5 D, i.e., 22% higher than the literature value of 5.3 D for Na on a clean Pt(111) surface [48,53]. This is excellent agree-

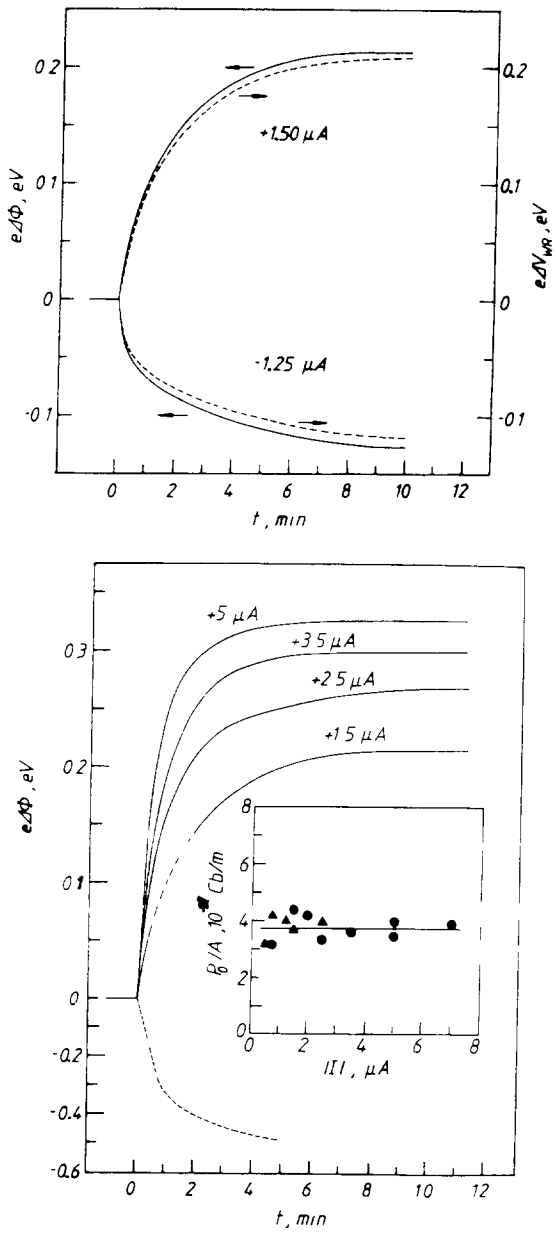

Fig 11 (a) Transient response of catalyst work function $e\Phi$ and potential V_{WR} upon imposition of constant currents I between the Pt catalyst (C2) and the Pt counter electrode, β''-Al_2O_3 solid electrolyte, $T=240°C$, $P_{O_2}=21$ kPa, Na ions are pumped to ($I<0$) or from ($I>0$) the catalyst surface at a rate I/F (b) Effect of applied current on induced work function change, dashed line catalyst C1, $T=291°C$, $P_{O_2}=5$ kPa, $P_{C_2H_4}=2.1\times10^{-2}$ kPa, solid lines catalyst C2, $T=240°C$, $P_{O_2}=21$ kPa, Insert Effect of applied current on computed initial dipole moment of Na on Pt, (●) $I>0$, (▲) $I<0$, [35]

ment, in view of the fact that in fig. 11 the Pt surface is essentially saturated in oxygen, which has been shown for systems like Cs/W(110) [54] and Cs/Ni(100) [55] to give P_0 values typically 20–30% higher than on the clean metal surface. As shown in fig 11 the computed P_0 value is independent of the magnitude and sign of the applied current which confirms the validity of the approach. One additional conclusion which may be drawn is that Na introduced on metal surfaces via β''-Al_2O_3 to induce NEMCA is not different from Na introduced as a dopant using standard metal dispenser sources [56]. An important advantage however in using the present approach, i e. in employing a solid electrolyte as the dopant donor is that the doping is reversible, i.e. the dopant can be removed electrochemically and that the amount and coverage of the dopant on the surface can be accurately determined by integrating eq. (22), i.e., by using Faraday's law.

When doped ZrO_2 is used as the ion donor then the situation is slightly more complicated, as the spillover oxygen anions may eventually form chemisorbed oxygen and desorb or react with the reactants, albeit at a slow rate [26,38]. Consequently the coverage of spillover oxygen anions is difficult to estimate and thus no reliable value for their dipole moments can yet be extracted.

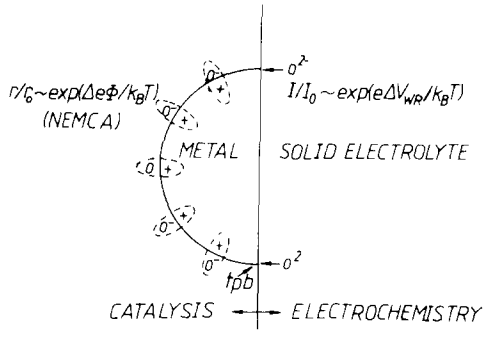

Fig 12 Origin of NEMCA and of eq (5) Upon polarization of the metal–solid electrolyte interface the catalyst potential changes by ΔV_{WR} and the catalyst surface work function by $\Delta e\Phi = e\Delta V_{WR}$ due to ion spillover, both the catalytic rate r and the electrocatalytic rate $I/2F$ are exponentially dependent on catalyst work function and potential change

6. Interpretation of the macroscopic features of NEMCA

The above theoretical considerations (section 4) and experimental findings (section 5) provide the framework for interpreting the general macroscopic features of NEMCA described in section 3

Thus, the exponential catalytic rate dependence on catalyst work function $e\Phi$ and the concomitant linear variation in catalytic activation energy with $e\Phi$ can be explained by taking into account the variation in the heats of adsorptions of reactants and intermediates with changing catalyst work function $e\Phi$ [26,38]. There is experimental evidence, e.g [38,49], also supported by some early electrostatic models [57] that over certain $e\Phi$ ranges the binding energy of chemisorptive bonds varies linearly with $e\Phi$. This can then explain both the observed linear dependence of activation energies on $e\Phi$ and the concomitant exponential catalytic rate dependence on $e\Phi$ as also analyzed in detail elsewhere [38].

The observation that the absolute value $|\Lambda|$ of the enhancement factor Λ is of the order of $2Fr_0/I_0$ (eq (5)) can be explained on the basis of fig 12 by noting that both r/r_0 and I/I_0 are exponentially dependent on $\Delta e\Phi/k_BT = e\Delta V_{WR}/k_BT$ [38].

Also the observation that NEMCA is due to ion spillover dipoles at the three-phase-boundaries at high activation overpotential (and not their surface diffusion on the catalyst surface) is the rate limiting step for the ion-compensating charge spillover, provides a direct explanation for the third general observation of NEMCA, i e., that the rate relaxation time constants are of the order of $2FN/I$ or $FN\theta_{Na}/I$, i.e. eqs (6) and (7)

7. Conclusions

Solid electrolytes can be used as ion donors or acceptors to control the work function of metal catalysts and to include dramatic and reversible changes in catalytic activity and selectivity. The present work provides a rigorous theoretical explanation for the observed one-to-one correspondence between ohmic-drop-free catalyst potential V_{WR} and catalyst surface work function $e\Phi$ The conclusion is that solid electrolyte cells with metal electrodes can be used both

to measure and to control the work function of the metal electrode surfaces. The latter observation provides a direct explanation for the NEMCA effect Direct in situ spectroscopic investigation of catalyst surfaces subject to NEMCA is highly desirable, as it could provide useful additional information about the exact nature of the spillover dipoles. The use of solid electrolytes for NEMCA, that is for in situ promotion of catalyst surfaces, allows for new areas of surface catalytic chemistry to be explored, and could lead to technological applications by influencing catalyst performance in desirable directions.

Acknowledgements

Financial support by the EEC Non-Nuclear Energy and JOULE programmes is gratefully acknowledged. One of the authors (CGV) also expresses his thanks to the Alexander von Humboldt Foundation of Germany for a Fellowship.

References

[1] C Wagner, Adv Catal 21 (1970) 323
[2] C G Vayenas and H Saltsburg, J Catal 57 (1979) 296
[3] C G Vayenas, Solid State Ionics 28–30 (1988) 1521
[4] M Stoukides, Ind Eng. Chem Res 27 (1988) 1745
[5] C G Vayenas, B Lee and J Michaels, J Catal 66 (1980) 36
[6] I V Yentekakis, S Neophytides and C G Vayenas, J Catal 111 (1988) 152
[7] S Pancharatnam, R A Huggins and D M Mason, J Electrochem Soc. 122 (1975) 869
[8] T M Gur and R A Huggins, J Electrochem Soc 126 (1979) 1067
[9] T M Gur and R A Huggins, Science 219 (1983) 967
[10] T M Gur and R A Huggins, J Catal 102 (1986) 443
[11] K Otsuka, S Yokoyama and A Morikawa, Chem Lett Chem Soc Japan. (1985) 319
[12] S Seimanides and M Stoukides, J Electrochem Soc 133 (1986) 1535.
[13] T Hayakawa, T Tsunoda, H Orita, T Kameyama, H Takahashi, K Takehira and K Fukuda, J Chem Soc Japan Chem. Commun. (1986) 961
[14] C G Vayenas and R D Farr, Science 208 (1980) 593
[15] C Sigal and C G Vayenas, Solid State Ionics 5 (1981) 569
[16] J N Michaels and C G Vayenas, J Electrochem Soc 131 (1984) 2544
[17] I V Yentekakis and C G Vayenas, J Electrochem. Soc 136 (1989) 996
[18] S Neophytides and C G Vayenas, J Electrochem Soc 137 (1990) 39
[19] C.G Vayenas, S. Bebelis and C Kyriazis, Chemtech. 21 (1991) 422
[20] M Stoukides and C G Vayenas, J Catal 70 (1981) 137
[21] M Stoukides and C G Vayenas, ACS Symp Ser 178 (1982) 181
[22] M Stoukides and C G Vayenas, J Electrochem Soc 131 (1984) 839
[23] C G Vayenas, S Bebelis and S. Ladas, Nature (London) 343 (1990) 625
[24] I V Yentekakis and C G Vayenas, J Catal 111 (1988) 170
[25] C G Vayenas, S Bebelis and S Neophytides, J Phys Chem 92 (1988) 5083
[26] S Bebelis and C G Vayenas, J Catal 118 (1989) 125
[27] S Neophytides and C G Vayenas, J Catal 118 (1989) 147
[28] H -G Lintz and C G Vayenas, Angew Chem 101 (1989) 725, Angew Chem Intl Engl Ed 28 (1989) 708
[29] C G Vayenas, S Bebelis, S Neophytides and I V Yentekakis, Appl Phys A 49 (1989) 95
[30] C G Vayenas, S Bebelis, I V Yentekakis, P Tsiakaras and H Karasali, Platinum Met Rev 34 (1990) 122
[31] C G Vayenas, S Bebelis and S Neophytides, in. New Developments in Selective Oxidation, eds C G Centi and P Trifiro, Studies in Surface Science and Catalysis 55 (Elsevier, Amsterdam, 1990) pp 643–652
[32] C G Vayenas and S. Neophytides, J Catal 127 (1991) 645
[33] C G Vayenas, S Bebelis and M Despotopoulou, J Catal 128 (1991) 415
[34] C G Vayenas, A Ioannides and S Bebelis, J Catal 129 (1991) 67
[35] S Ladas, S Bebelis and C G Vayenas, Surface Sci 251/252 (1991) 1062
[36] C G Vayenas, S Bebelis, I V Yentekakis, P Tsiakaras, H Karasali and Ch Karavasilis, ISSI Lett 1 (1991) 5
[37] S Bebelis, Ch Karavasilis, H Karasali, P Tsiakaras, I V Yentekakis and C G Vayenas, in Proc 2nd Intern Symp on Solid Oxide Fuel Cells, Athens, Greece (Publ EEC, Luxembourg, 1991) pp. 353–360
[38] C G Vayenas, S Bebelis, I V Yentekakis and H -G Lintz, Non-Faradaic Electrochemical Modification of Catalytic Activity A Status Report Catalysis Today (Elsevier, Amsterdam, 1991), to be published
[39] C G Vayenas, S Bebelis and C Kyriazis, Chemtech 21 (1991) 500
[40] J Pritchard, Nature (London) 343 (1990) 592
[41] W L Worrell, in Electrochemistry and Solid State Science Education, eds W R Smyrl and F McLarnon (The Electrochem Soc , Pennington, NJ, 1986)
[42] B C H. Steele, in Electrode Processes in Solid State Ionics, eds M Kleitz and J Dupuy (Reidel, Dordrecht, 1976) p 367
[43] E J H Schouler and M Kleitz, J Electrochem Soc 134 (1987) 1045
[44] J O 'M Bockris and A K N Reddy, Modern Electrochemistry, Vol 2 (Plenum Press, New York, 1970)

[45] H J Reiss, J Phys Chem. 89 (1985) 3783
[46] H J Reiss, J Electrochem Soc 135 (1988) 247c
[47] P M Gundry and F C. Tompkins, in Experimental Methods in Catalytic Research, ed R B Anderson (Academic Press, New York, 1968) pp. 100–168
[48] J Hölzl and F K Schulte, Solid Surface Physics (Springer, Berlin, 1979) pp 1–150
[49] S Trasatti, in Advances in Electrochemistry and Electrochemical Engineering, Vol 10, eds H Gerischer and Ch W Tobias (Wiley, New York, 1977)
[50] C Lamy, in Propriétés Électriques des Interfaces Chargées, ed D Schumann (Masson, Paris, 1978) pp 210–241
[51] T Arakawa, A Saito and J Shiokawa, Chem Phys Lett 94 (1983) 250
[52] T Arakawa, A Saito and J Shiokawa, Appl Surface Sci 16 (1983) 365
[53] W Schroder and J Holzl, Solid State Commun 24 (1977) 777
[54] J L Desplat and C A Papageorgopoulos, Surface Sci 92 (1980) 97
[55] C A Papageorgopoulos and J M Chen, Surface Sci 52 (1975) 40
[56] H P Bonzel, Surface Sci Rep 8 (1987) 43
[57] M Boudart, J Am Chem Soc 74 (1952) 3556